Eur Radiol (2007) 17: 2767–2779
DOI 10.1007/s00330-007-0651-9

Willi A. Kalender
Yiannis Kyriakou

Flat-detector computed tomography (FD-CT)

Received: 15 December 2006
Revised: 20 February 2007
Accepted: 30 March 2007
Published online: 23 June 2007

W. A. Kalender (✉) · Y. Kyriakou
Institute of Medical Physics,
University of Erlangen-Nuernberg,
Henkestr. 91,
91052 Erlangen, Germany
e-mail: willi.kalender@imp.uni-erlangen.de
url:www.imp.uni-erlangen.de
Tel.: +49-9131-8522310
Fax: +49-9131-8522824

Abstract Flat-panel detectors or, synonymously, flat detectors (FDs) have been developed for use in radiography and fluoroscopy with the defined goal to replace standard X-ray film, film-screen combinations and image intensifiers by an advanced sensor system. FD technology in comparison to X-ray film and image intensifiers offers higher dynamic range, dose reduction, fast digital readout and the possibility for dynamic acquisitions of image series, yet keeping to a compact design. It appeared logical to employ FD designs also for computed tomography (CT) imaging. Respective efforts date back a few years only, but FD-CT has meanwhile become widely accepted for interventional and intraoperative imaging using C-arm systems. FD-CT provides a very efficient way of combining two-dimensional (2D) radiographic or fluoroscopic and 3D CT imaging. In addition, FD technology made its way into a number of dedicated CT scanner developments, such as scanners for the maxillo-facial region or for micro-CT applications. This review focuses on technical and performance issues of FD technology and its full range of applications for CT imaging. A comparison with standard clinical CT is of primary interest. It reveals that FD-CT provides higher spatial resolution, but encompasses a number of disadvantages, such as lower dose efficiency, smaller field of view and lower temporal resolution. FD-CT is not aimed at challenging standard clinical CT as regards to the typical diagnostic examinations; but it has already proven unique for a number of dedicated CT applications, offering distinct practical advantages, above all the availability of immediate CT imaging in the interventional suite or the operating room.

Keywords Computed tomography · Angiography · Interventions · Flat detectors · C-arm systems

Introduction

The development of flat-detector (FD) technology originally aimed at improving standard radiography by providing higher absorption efficiency and a wider dynamic range than available with X-ray film or film-screen combinations. Direct digital read-out and frame rates of several images per second offer additional practical advantages and also the possibility for fluoroscopic examinations. The introduction of FD technology was announced and expected for the 1990s; it was delayed due mostly to production problems, but is now generally available.

For several years this new detector technology has been under investigation also for standard X-ray computed tomography (CT) applications and under evaluation for new and dedicated scanner design. Nevertheless, in most cases today the term FD-CT refers to CT imaging using C-arm systems built for radiography and fluoroscopy which are equipped with an FD and prepared to take projection data over an angular range of 180° or more.

The basic idea to acquire projection data over a typically 180°-plus fan angle was already pursued in the 1990s [1–4]. The early work was conducted on C-arm systems equipped with conventional image intensifiers (Fig. 1a). Like CT detector systems, image intensifiers offer a very limited performance, due above all to low dynamic range, image distortions and potential influences of changing magnetic interferences during the rotational movement. This prevented the use of such systems for CT-like applications in the classical sense, i.e. the imaging of soft-tissue structures. Image intensifier-based C-arms were typically only used for high-contrast vessel imaging and mostly employed intra-arterial injections. They provided good high-resolution imaging at contrast levels even exceeding 1,000 Hounsfield units (HU), as shown by the example in Fig. 1b. Respective commercial solutions with several hundred clinical installations were widely used. It is foreseeable, however, that they will be replaced by FD-based C-arm CT systems (Fig. 1c), which offer higher dose efficiency, higher image quality and, to a good approximation, CT-like performance. In particular, they provide the possibility for assessing soft-tissue structures, as shown by the example in Fig. 1d.

Modern C-arm CT systems presently find rapid acceptance since they offer improved image quality, versatility and dedicated applications for planning, guiding, monitoring and assessing interventional procedures [5–12]. These are above all their use in interventional procedures and in intra-operative imaging. The physical and technical characteristics of such systems, the trade-off between image quality and dose in comparison with standard clinical multi-slice spiral CT (MSCT) systems with dedicated CT detectors shall be the focus of this review. Image intensifier-based systems are not included; however, the review is complementedby an overview of novel types of dedicated CT scanner designs using FD technology. Future aspects and potential developments of FD technology and FD-CT are also discussed.

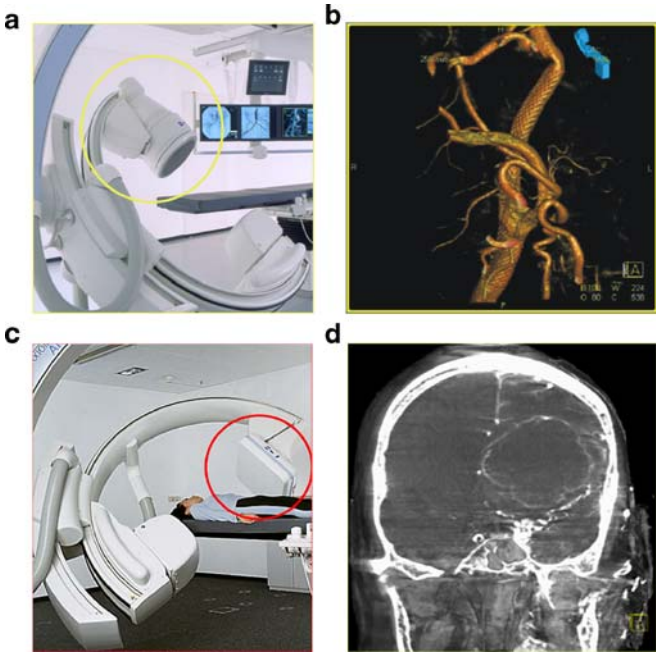

Fig. 1a–d CT imaging using C-arm systems equipped with area detectors has been pursued for many years already. **a** Initially, image intensifiers (II) were used which were limited to high-contrast vascular imaging after intra-arterial injection; **b** an II-CT of a stented carotid artery. Modern FD technology, here a 30×40 cm^2 FD, which can be rotated in portrait and landscape format (**c**), allows for better image quality and thereby also for soft tissue delineation; **d** for a cystic ring-enhancing glioma of the left hemisphere

Technology of C-arm FD-CT systems

The main components of C-arm FD-CT systems to be considered in this section are the X-ray source, the X-ray detector, the mechanical set-up, and the image reconstruction unit. Many aspects of the discussion below apply just the same to the dedicated FD-CT systems presented later; particulars of such systems will be discussed there whenever indicated.

X-ray sources

C-arm systems have been designed and are generally used for fluoroscopy; the CT option at present is an addition to the existing system. Accordingly, we are faced with the standard X-ray sources typically used in angiography, interventional or intra-operative imaging. Performance parameters available and typically chosen differ slightly from those commonly used in clinical CT. Smaller focal spot sizes are available, the power levels and the high voltage values are lower. Typical parameters for C-arm CT and clinical CT are given in Table 1 for comparison.

C-arm systems offer exposure control schemes both for radiography and fluoroscopy as a standard. This involves not only an adaptation of the tube current but also of the tube voltage. In CT, a variation of the tube voltage with projection angle is undesirable since the attenuation values will change when the beam energy changes; inconsistent measurements of attenuation and, in consequence, image artefacts would result. Therefore FD-CT is generally carried out with fixed voltage as is the case in clinical CT; automatic exposure control (AEC) modulates the tube current only and aims to achieve constant detector entrance dose over the scan range [13, 14].

Detector technology

FD technology was initially developed for radiography and later for angiography in order to overcome insufficiencies of X-ray film and image intensifiers. The intent was to

Table 1 Typical parameters for MSCT and FD-CT

	MSCT	FD-CT
Tube voltage	80–140 kV	50–125 kV
Tube current	10–600 mA	10–800 mA
X-ray power	20–100 kW	10–80 kW
Focal-spot size	0.6–1.2 mm	0.3–0.8 mm
Rotation time	0.33—1 s	5–20 s
Detector elements		
- in fan direction	512–1,024	512–2,490
- in z-direction	16–64	512–2,490
Field of measurement		
- in fan direction	500–700 mm	100–250 mm
- in z-direction	2–40 mm	100–200 mm
Min. slice thickness	0.6 mm	0.1–0.3 mm
Typ. scintillator/thickness	Gd_2O_2S/1.0–1.4 mm	CsI:(Tl)/0.4–0.8 mm
Data rate	≤1,000 MB/s	≤60 MB/s

provide fast and repeated direct digital readout and higher dynamic range. The basic design principle nevertheless still relies on the conversion of X-rays to light: a fluorescence scintillator screen, mostly a caesium iodide substrate, is used as an X-ray converter. The light emitted is recorded by a regular array of photodiodes placed in immediate contact with the fluorescent screen (Fig. 2a). Typical design parameters of FDs are included in Table 1.

The selection of the entrance screen material and thickness, i.e. the X-ray sensor characteristics, is governed by the same criteria as in screen-film radiography. Greater thicknesses mean higher absorption efficiency; however, at the same time spatial resolution is degraded since the light photons are emitted in all directions and propagate diffusely (Fig. 2b). Special efforts were directed at developing and manufacturing structured needle-type phosphors which guide the light along these structures. These efforts have brought substantial improvements. Nevertheless, light is not guided perfectly along the needles and there is still a degradation of spatial resolution. Therefore, screen thicknesses which offer lower absorption than in clinical CT are generally chosen. In any case, spatial resolution today is ultimately limited by the fluorescence screen, even if very small pixel sizes defined through larger photodiode matrices become available.

In consequence, efforts have been directed at so-called direct converters that allow the convertion of X-ray photons directly to electron charge, which then travels along the direction of an applied electric field and is collected without a significant loss of resolution (Fig. 2b *right*). Directly converting materials such as selenium [15] or mercuric iodide [16, 17] are not yet commercially available for CT imaging purposes, however; in particular, they also do not provide the necessary temporal characteristics and dynamic capabilities [18, 19].

FDs are available in formats typically from 5×5 cm^2 up to 40×40 cm^2; the selection will depend on the application and on cost considerations. The production of large FDs has proven difficult and costly due to frequent pixel defects. The typical dynamic ranges of 10–14 bits again are adequate for radiography and fluoroscopy. For CT applications, higher values would be desirable. Also, the geometric efficiency for indirect converters is limited. For pixel sizes of 150-μm pitch the fill-factor amounts to approximately 65%; for smaller pixels, the geometric efficiency decreases further. Direct converters do not suffer from this limitation.

Temporal response was no major concern in the design and development of FDs. Frame rates of 5–10 images per second are typically available today for full matrix readout which appears adequate for most fluoroscopic applications. Combining of pixels, the so-called binning process, allows for higher readout rates, e.g. up to 60 images per second with 4×4 binning, but at the expense of resolution (see *Spatial resolution* in the next section). For CT purposes, an increase would be of interest, but only if the characteristics of the absorber are also adequate [20]. Caesium iodide was abandoned in the 1980s in clinical CT since its temporal lag phenomena classified it insufficient for fast CT [13, 21, 22]. The ideal detector is still to be developed.

Mechanical set-up

C-arm systems are characterized by flexibility in their use; in particular, by the possibility of choosing arbitrary angulations. The most important additional demand imposed by CT scanning is to allow for a circular scan over at least 180°. For high image quality, a minimum angular range of 180°-plus fan angle is required. An additional requirement is related to mechanical stability: for good CT image quality exactly the same object section has to be viewed for all projections. This means that the desired perfect planar trajectory of focus and detector has to be realized with very high precision. Otherwise the attenuation data measured for different projection angles will be inconsistent. Visible artefacts will result even for minute deviations if such misalignment remains uncorrected; an example including corrections is given in the next section under *Artefact considerations*.

Grids are generally available on C-arm systems but there is no consensus yet when they should be applied in CT scanning. Effects of scattered radiation on image quality are discussed further under *Artefact considerations* in the next section.

Image reconstruction

FD-CT can be viewed as synonymous to cone-beam CT, which demands special efforts at image reconstruction. The

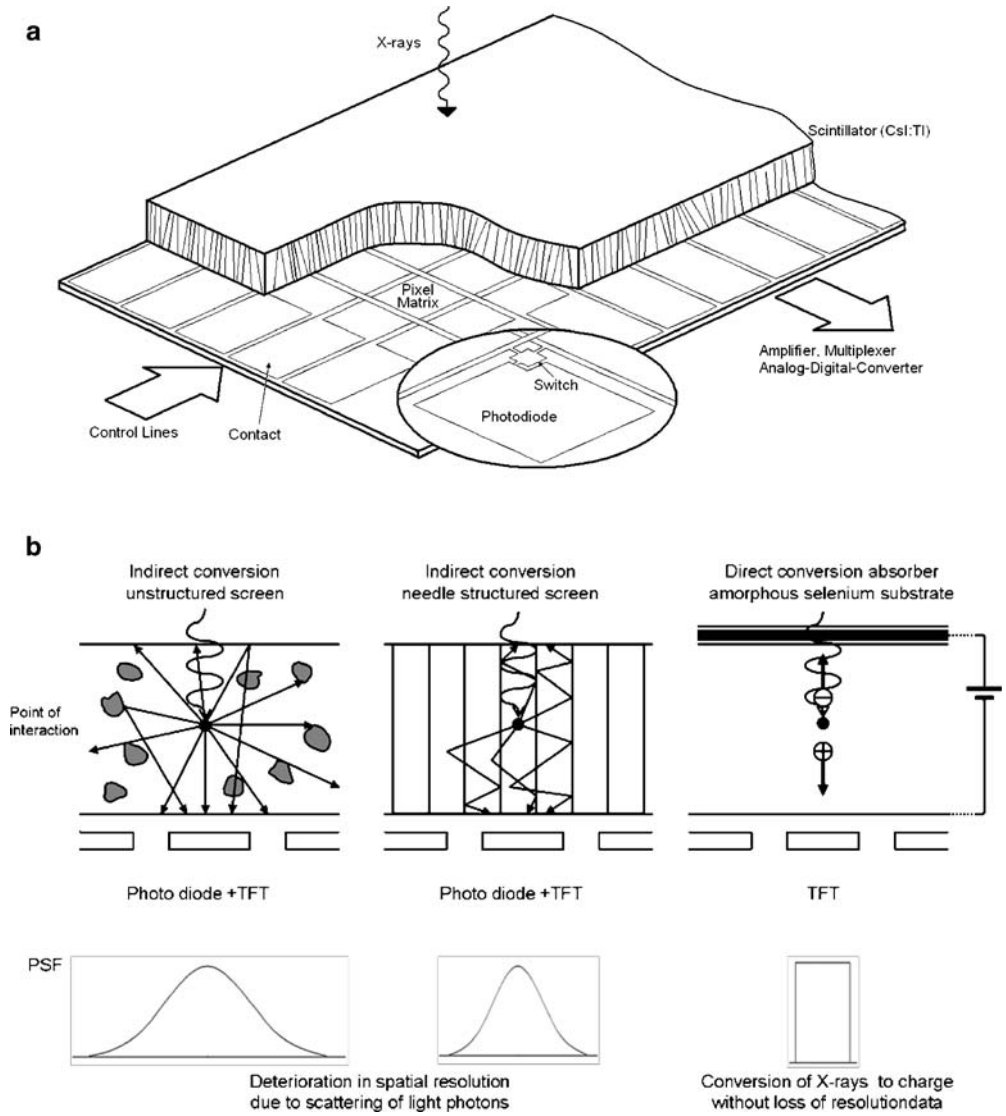

Fig. 2a, b Typical set-up of an FD. A caesium iodide fluorescence screen serves as an X-ray to light converter. **a** The light photons are recorded by an array of photodiodes which typically define pixels of 100–200 μm in size. **b** *left* Light diffusion inevitably leads to a degradation of resolution. **b** *centre* This effect can be reduced significantly when using structured crystals, **b** *right* but only materials which directly convert charge to electric signal avoid this effect

standard convolution-backprojection approaches only work with high image quality when a perfect planar or fan-beam geometry is given. When the detector extent in the z-direction is increased, the cone angle, κ, increases just the same from 0° to typically 5–20°. For clinical CT, it has been shown that up to 64 slices, corresponding to about 2–4° cone angle, approximate reconstruction approaches such as the so-called advanced single-slice rebinning (ASSR) algorithms applied to spiral CT scan data provide excellent image quality [23].

For wider cone angles and for circular scan trajectories the situation is complicated. The reconstruction approach of choice is the so-called Feldkamp algorithm [24]. Its performance varies slightly with the type of implementation, reconstruction times are typically 2–10 min for an image volume of 512^3. In principle, high image quality can only be guaranteed for the central plane. Image quality will be degraded for areas outside the central plane, and the degradation will increase as a function of the distance to it. The artefacts are generally called cone-beam artefacts [13, 24, 25]. Work on so-called exact cone-beam reconstruction using complete trajectories is ongoing. It is not of immediate importance for routine daily work.

Image quality and dose in C-arm FD-CT

Values and images presented in this section were obtained with a standard FD of 1,920×2,490 detector elements with 154-μm pixel dimensions, 30×40 cm^2 entrance field and geometry as given in Table 2. These results shall only serve as examples to illustrate the general statements. It has to be noted that statements regarding image quality will also depend on the parameter and conditions chosen, such as the object or phantom size, the X-ray spectrum, or the specific application.

Table 2 C-arm FD-CT parameters used in generating the data for Figs. 3 and 4

Tube voltage	70 kV (head scans); 125 kV (body scans)
Distance focus rotation centre	785 mm
Distance focus detector	1,200 mm
Detector entrance field	30×40 cm^2
Pixel size	154 μm
Scintillator	0.6 mm CsI(Tl)
Angular increment	0.4° (2×2 binning), 1.2° (no binning)
Angular range	200°

Spatial resolution

Similar to clinical CT, spatial resolution depends on focal spot size, detector element size, the geometry and the reconstruction parameters [13]. The parameter modified most easily is the detector element size: it is enlarged effectively by binning. A binning of $n \times n$ means that $n \times n$ pixels are combined and read out as one. Binning reduces noise and the amount of data and thereby can increase frame rates, but it also reduces spatial resolution, as shown by modulation transfer function (MTF) and bar pattern measurements. The 10% MTF values amounted to 3.0 lp/mm with no binning and 1.5 lp/mm with 2×2 binning, respectively (Fig. 3a); visual evaluation of a bar pattern phantom confirms these results (Fig. 3b). In any case, this exceeds the spatial resolution of MSCT, which typically provides up to 1.2–1.4 lp/mm for high-resolution modes.

Noise, contrast and contrast resolution

Soft-tissue or, in general, low-contrast resolution is strongly dependent on image noise levels. FDs still are less efficient than detectors used for MSCT and are thus expected to provide higher noise and reduced low-contrast resolution at a given dose level. Figure 4 shows reconstructions for a low-contrast phantom with spheres of different diameters ranging from 5–20 mm with contrast levels of 10 and 20 HU. Figure 4a,b shows the result of a reconstruction at the same dose level but at different resolution levels. Figure 4a provides high spatial resolution but also higher noise and decreased low-contrast detectability; a smooth reconstruction kernel and a larger slice width were chosen for Fig. 4b. The trade-off between spatial resolution and noise is further explained below (see *General considerations regarding resolution and dose*). The effect of increased dose which leads to a decrease of image noise is indicated in Fig. 4c. At a weighted CT dose index ($CTDI_w$) value of 5.9 mGy, 10-mm spheres at 10 HU contrast are resolved for a slice thickness of 1 mm.

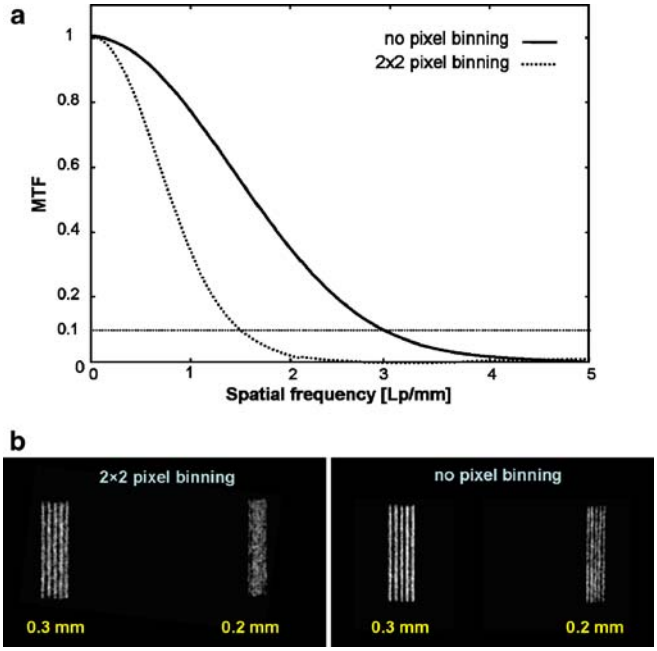

Fig. 3 Superior spatial resolution is demonstrated **a** by MTF and **b** by bar pattern measurements. Pixel binning (see text) has a strong effect, but resolution generally exceeds that of clinical CT

Dose considerations

Dose considerations for FD-CT are largely the same as in MSCT, and all general recommendations apply to both in an analogous manner [13]. The analogy also holds for problems in dose assessment which have evolved lately. The generally accepted technical dose descriptor for CT systems is the CT dose index (*CTDI*)

$$CTDI = \frac{1}{M \cdot S} \int_{-50mm}^{50mm} D(z)dz \neq \frac{1}{M \cdot S} \int_{-\infty}^{\infty} D(z)dz \qquad (1)$$

It was defined in the 1980s, when only low z-coverage scans were available, and intended to give a correct estimate of the integrated dose resulting from a given single

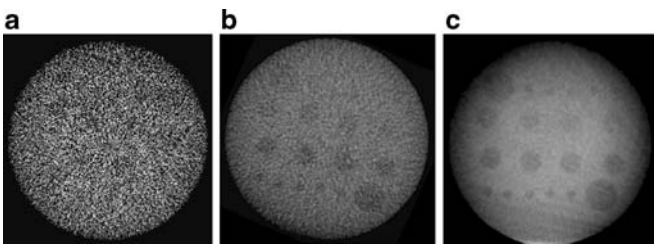

Fig. 4a–c The detectability of low-contrast details depends on reconstruction parameters and dose. **a**, **b** High- and low-resolution reconstructions are associated with high and low noise, respectively. **c** An increase of dose, compared with **a**, **b**, leads to lower noise and results in improved low-contrast detectability (see text)

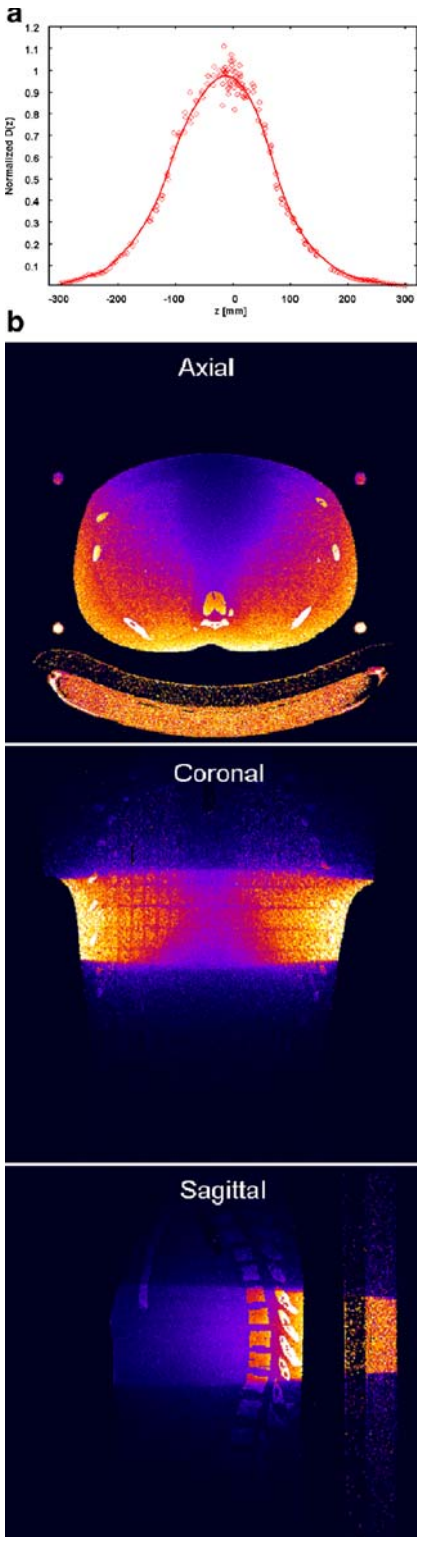

Fig. 5a, b Dose in FD-CT. **a** Dose profile along the central axis of a 600-mm long PMMA phantom of 32-cm diameter for 200-mm z-collimation. **b** Dedicated Monte Carlo tools provide exact 3D dose distributions for any CT scan and scan parameters

scan for a range of 14 slice widths, *S*, [26] and later for 100 mm along the dose profile, *D*(z) [13]. With the advent of multi-slice systems with collimations $M \cdot S$ of 20–120 mm in MSCT and up to 200 mm in FD-CT [given at the centre of rotation (COR)] the *CTDI* definition is not adequate any more [12, 27, 28]. The same statement holds for the weighted $CTDI_w$, which is defined as $CTDI_w = 1/3 \cdot CTDI_c + 2/3 \cdot CTDI_p$, where $_c$ and $_p$ denote central and peripheral positions in the phantom. Analogously, the standard measurement methods using an ionization chamber of 100 mm length will provide an insufficient estimate of the delivered dose. Figure 5a shows that dose profiles measured with thermoluminescence dosimeters (TLD) in the centre of a body CTDI phantom of 32 cm diameter and 600 mm z-extent extend far beyond the 100 mm range. Using such extra-long phantoms and ionisation chambers is not practical. Standard CTDI phantoms and ionisation chambers with a length of 150 mm and 100 mm, respectively, which are generally used today, offer a poor approximation only and are a cumbersome exercise [26, 29]. Comparisons of modern CT systems, including their dose characteristics, are still difficult at present and a consensus on how to do it is still to be found.

For system comparisons in this paper, we performed the corresponding dose integral measurements with a 25-cm ionization chamber in order to calculate the $CTDI_w$ values providing an approximate dose indicator. We propose using Monte Carlo (MC) calculations [13, 30] for phantom- or patient-specific dose assessment of both integral dose values and dose distributions. Figure 5b shows the dose distribution for a thorax cross-section obtained by a C-arm FD-CT scan over 200° with the tube travelling beneath the patient table. When combined with point measurements (e.g. air kerma at the COR) simulations provide quantitatively correct dose distributions. The MC simulation tool is more flexible than any measurement setup, and the calculation of 3D dose distributions can be easily adapted to scan parameters, spectra, geometries and also to tube current or voltage modulations to be developed in the future [13].

Artefact considerations

FD-CT scanners face problems such as beam hardening, defect detector elements or metal artefacts like any other X-ray CT imaging system. Due to their special geometry and mechanics characterized by smaller fan angles, larger collimation in z-direction, and mechanical instabilities, FD-CT scans additionally have to deal with data truncation, high scatter intensities and misalignment artefacts.

The field of measurement (FOM) for FD-CT scanners is limited to about 250 mm (see Table 1), which is smaller than the 50 cm FOM necessary for standard body scans. So-called data truncation artefacts result, which influence the CT-value accuracy and disturb the diagnostic quality of the images. Correction algorithms [31, 32] allow to restore

Table 3 Quality indices according to equation (2) for MSCT and FD-CT

	Phantom	Tube voltage (kV)	Q
MSCT	Head	80	1.00
FD-CT	Head	70	0.94
MSCT	Body	120	1.00
FD-CT	Body	125	0.37

image quality and improve the accuracy of the CT values in the FOM. The application of such "detruncation" algorithms also provides anatomic information outside the FOM. Although image quality is impaired, this can be useful in some situations.

The increased collimation in the z-direction results in increased scatter fractions [33–35]. This will induce severe cupping artefacts, i.e. a CT value drop towards the centre of the phantom. Both the use of an anti-scatter grid and of scatter correction algorithms yield a more homogeneous display and improved CT value accuracy. Nevertheless, the use of anti-scatter grids is not generally accepted [10], since their employment results in a dose penalty. An increase of mA values is necessary to make up for their absorption of primary photons. The use of anti-scatter grids in FD-CT is generally considered beneficial in the case of large objects since these are accompanied by high scatter fractions [10].

Mechanical stability is an important issue for C-arm based FD-CT systems. Unlike conventional CT gantries, the C-arm movement and consequently the respective detector-source positions for each projection may be afflicted with an unacceptably high inaccuracy or misalignment depending on the trajectory, rotation speed etc. [36]. Typical effects of misalignment in the reconstructed images are a deformation of fine structures and a generally reduced image quality; correction techniques based on offline [37, 38] or online calibration procedures [39] usually provide removal of misalignment artefacts to a high degree.

General considerations regarding resolution and dose

The general considerations of this section shall serve to give a combined assessment of spatial resolution, low-contrast resolution, noise and the delivered dose in a single quality factor which characterizes a CT system. It is valid both for conventional spiral CT and FD-CT systems and enables a direct comparison of modalities.

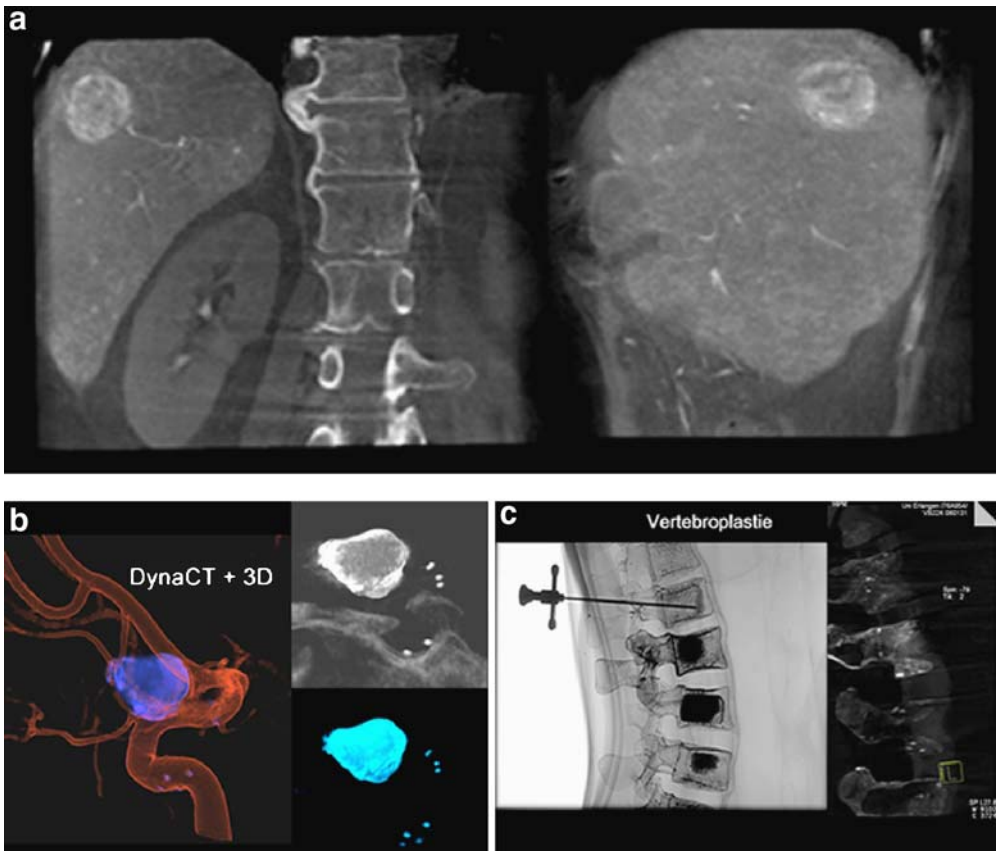

Fig. 6 Clinical FD-CT applications. (**a**) Embolisation of a liver tumour (*left*: coronal; *right*: sagittal view). **b** FD-CT/angiographic CT after stent-assisted coil embolization of a wide-necked paraophthalmic internal carotid artery aneurysm. (**c**) Vertebroplasty in an in-vitro model. Plain radiography (*left*) and FD-CT (*right*)

The quality factor Q is defined [13] as

$$Q = c \cdot \frac{1}{\sigma^2 \cdot \rho_{10\%}^{-4} \cdot D} \quad (2)$$

where c is usually chosen such that the Q-value for the system chosen as reference in a comparison is set equal to 1. Noise is given by σ, which is the standard deviation of the CT values in a homogeneous phantom section, $\rho_{10\%}$ is the 10% MTF-value representing a spatial resolution measure, and D an indicator for the delivered dose. Isotorpic resolution is assumed, otherwise the chosen slice thickness, S, would have to be included explicitly [12].

Table 3 shows an exemplary comparison of clinical CT to C-arm flat-panel CT for standard head and body scans. In this case D is represented by the $CTDI_w$ value for the corresponding scan for a head (16 cm) and a body (32 cm) CTDI-phantom, respectively. For the head scan with low X-ray energy, FD-CT is almost as efficient as MSCT; for the body phantom at higher attenuation and X-ray energy, FD-CT is inferior. This is to be acknowledged as a fact, but generally is not a problem since interventions and not diagnoses are the goals of the examination.

The acknowledged advance offered by FD-CT with respect to image quality is the improved spatial resolution. In many applications, for example in imaging stents during the intervention, this is a particular advantage. In most other respects, image quality lower than in clinical CT is accepted. Artefacts due to cone-beam acquisition and the limited field of measurement are visible in many cases (see Fig. 6), but it is of no major relevance: for the task at hand it is fully sufficient. This is a statement valid for many, if not most, FD-CT applications. When coiling a cerebral aneurysm, the interventional radiologist needs the possibility of an immediate CT control scan when a complication such as a rupture is suspected. The specific application, patient handling and safety and workflow are the dominant considerations.

For a given level of image quality, dose requirements are higher for FD-CT than for clinical CT due to the lower detection efficiency. However, in most applications the mAs product per single scan is much lower for FD-CT. It has to be kept in mind, however, that repeated scans may be the case. Cumulated dose, including the contributions from fluoroscopy or single radiographs, can vary widely, and a general specification of dose values is not possible.

One further aspect regarding image quality should be noted for chest and abdominal examinations: due to the slow rotation of the FD-CT patient, motion will often reduce spatial resolution.

Novel implementations and applications of FD-CT

The availability of FD technology for CT imaging has stimulated a surprising number of novel developments for clinical, pre-clinical, animal and in vitro imaging. Routine interventional and intraoperative imaging are the primary examples. Additionally, we here give a brief overview of further innovative developments of FD-CT to inform and to alert the reader to these.

C-arm-based interventional FD-CT

FD-CT image-guided tumour therapy is one of the fastest growing applications in radiology; it applies to all body regions and includes tumour embolisation (Fig. 6a) and radiofrequency ablation. Vascular interventions for treatment of aneurysms and arteriovenous malformations, stent imaging and angioplasties are also growing in importance. Angiographic FD-CT is particularly helpful during neurointerventional procedures, i.e. intracranial stenting for cerebrovascular stenoses, stent-assisted coil-embolization of wide-necked cerebral aneurysms (Fig. 6b) and embolizations of arteriovenous malformations of the brain [39, 40]. Especially, the small intracranial stents hardly visible in plain fluoroscopy can be visualized well using high-resolution FD-CT. Additionally, by providing morphologic images of the brain within the angio suite FD-CT is able to work up periprocedural hemorrhage in the rare cases of intraprocedural aneurysm or AVM rupture and may thus significantly improve immediate complication

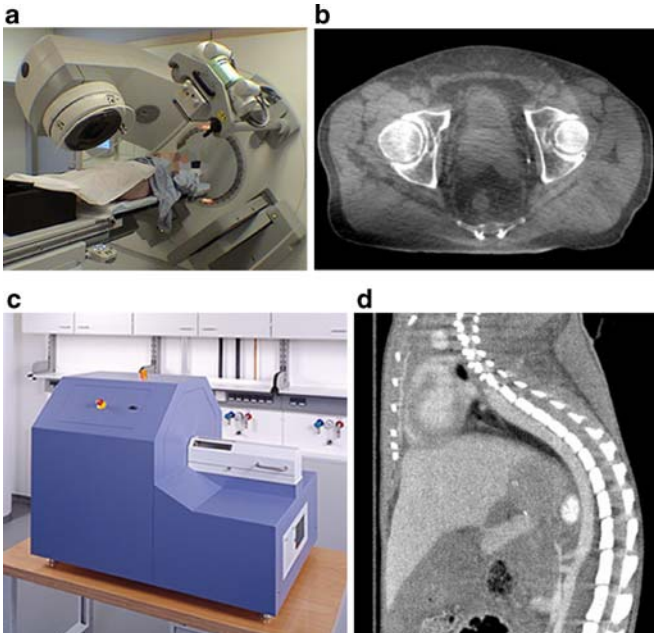

Fig. 7a–d Dedicated FD-CT scanners. **a**, **b** X-ray source and FD attached to a rotating linear accelerator for CT imaging of radiotherapy patients on the treatment couch. (Courtesy of D. Jaffray, Toronto.) **c** Micro-CT scanner for fast low-dose in-vivo imaging of small animals. **d** A 90-s scan of a mouse at 80-μm resolution and 130 mGy after contrast medium injection

management without the need to transfer the patient to the CT suite [40–42]. Spinal interventions such as kyphoplasty or vertebroplasty (Fig. 6c) also benefit from FD-CT. It has to be noted that FD-CT benefits for soft-tissue interventions and imaging without contrast medium application have not yet been evaluated completely.

C-arm-based intra-operative FD-CT

Intra-operative imaging has also shown an impressive upward trend over the past few years. It is focused on orthopaedic and trauma surgery, such as joint replacements and spine surgery. Similar to the situation in the interventional suite, FD-CT allows immediate and conclusive control of the surgical intervention, as for example the correct placement of screws without impairment of joint function.

FD-CT in combination with radiation therapy units

Attaching a standard X-ray tube and an FD to a rotating linear accelerator allows for CT imaging of the patient on the therapy couch [9, 43, 44]. It is the same rationale as in C-arm CT: the practical advantages of real-time control of patient positioning and tumour control and the option of real-time therapy planning outweigh potential disadvantages in image quality, which are to be acknowledged (Fig. 7a,b). The demanding diagnostic work-up has usually been completed earlier by clinical CT or another modality; FD-CT image quality is adequate to accomplish the task at hand.

FD-CT for dedicated maxillo-facial scanning

Imaging of the maxillo-facial skull has received growing attention in the past years as the number of image-guided procedures in dental and maxillo-facial surgery, in

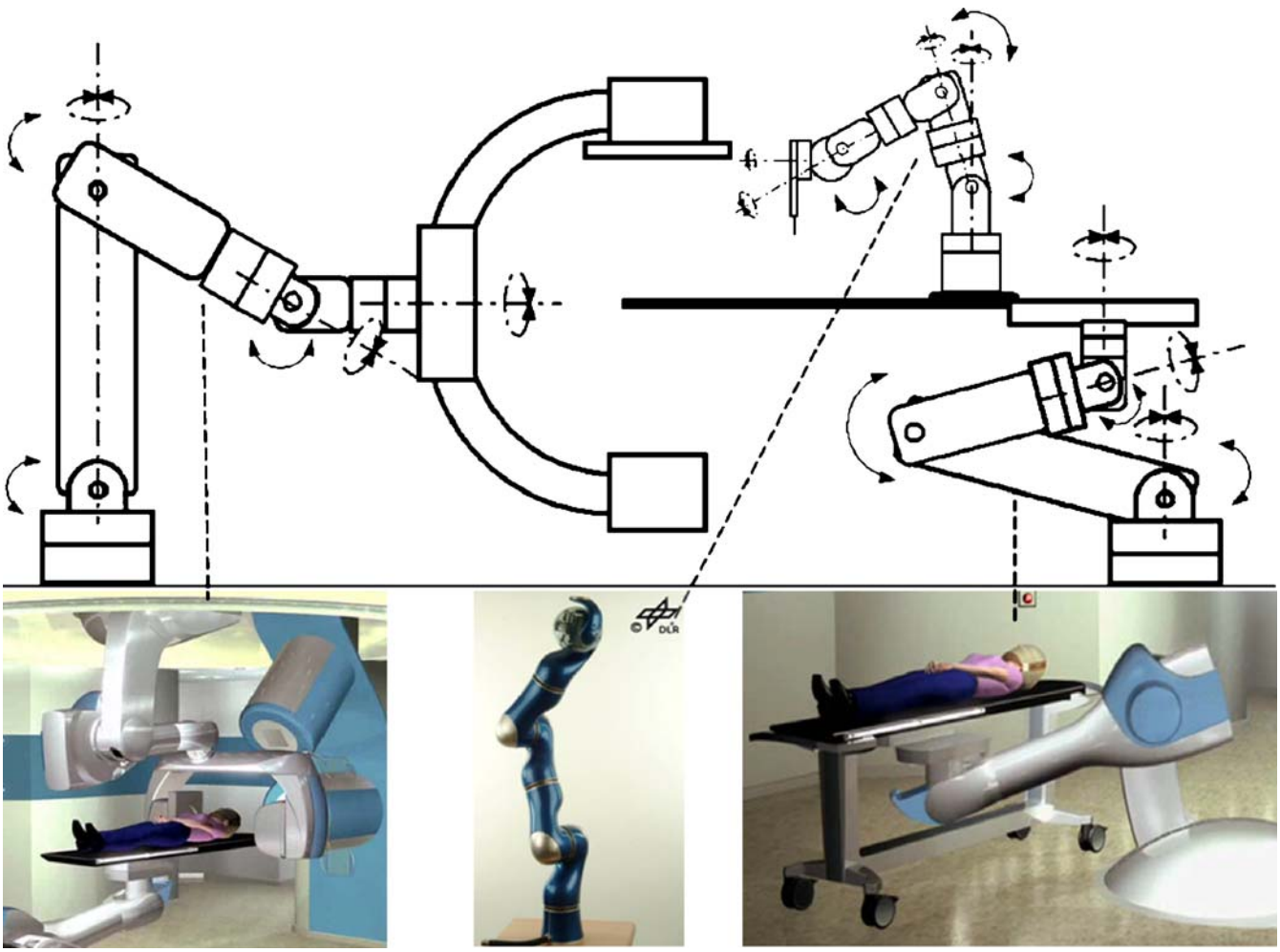

Fig. 8 Potential future developments in FD-CT: robots will allow for faster, more precise and more flexible data acquisition and therapy (see text). (Renderings of the two large robots are a courtesy of Siemens Medical Systems Particle Therapy Division)

particular dental implants, is increasing. Respective dedicated scanners were initially equipped with image intensifiers; image quality was very limited, the exposure unnecessarily high [45]. Although better results are obtained at lower dose when using standard clinical CT scanners with appropriate scan protocols, the high interest of practitioners in that field led to the installation of hundreds of maxillo-facial scanners all over Europe. The introduction of FD technology into such scanners has improved the situation. Although the relation of image quality to patient dose is still inferior to what MSCT can offer, workflow considerations and the desire to control the CT imaging part in dental maxillo-facial procedures appears to be the dominant consideration.

FD-CT for dedicated imaging of the breast

CT imaging of the female breast was a topic for a short time in the 1980s [46], but it never got established. Spatial resolution was insufficient at the time, and dose levels were significantly higher than in standard mammography. At present, new efforts are under way using dedicated FD-CT scanner set-ups, which expose the female breast only [47]. The patient is positioned prone on a table with one breast at a time in the field of measurement. Since exposure of the complete thorax is avoided, lower kV and mAs settings are possible than in standard CT. There is agreement with respect to the finding that CT imaging at an adequate image quality level can be achieved by such scanners at a dose level which is equivalent to two-view standard mammography [47–49]. The major challenge for this FD-CT application is not image quality, but patient positioning to ensure that the breast is imaged completely. First results are promising nevertheless.

FD-CT in combination with conventional CT gantries

Last, but not least, FD technology has also been integrated in standard CT designs [50–53]. Respective efforts were labelled experimental and aimed at exploring so-called "volume CT" options. At present they aim at pre-clinical imaging applications. It remains open if such designs will become acceptable for clinical CT; this will above all demand the development of FD designs improved with respect to dose efficiency and speed. In any case, such scanners are associated with high cost and the demand for a dedicated CT room, which is a disadvantage for most pre-clinical research laboratories.

FD-CT for high-resolution micro-CT imaging

First efforts at micro-CT imaging, i.e. CT imaging at spatial resolution levels typically between 5 and 100 μm, date back to the 1980s. A variety of detectors, such as one-dimensional linear arrays, fluorescence screens coupled optically to a photodiode array or image intensifiers, were in use. The advent of FD technology has added momentum to developments and research in this field. Micro-CT also received increasing attention due the augmented interest in molecular and small-animal imaging (SAI). Dedicated in-vivo SAI scanners resemble clinical CT scanners with the animal on a movable bed and the gantry rotating around it. They are self-shielded in most cases, often in desk-top design, and do not require any special building preparations (Fig. 7c). Scan times vary widely between 30 s to more than 20 min. For the faster scanners, even CT angiography has become possible routinely (Fig. 7d).

Potential future developments

The field of FD-CT is still comparatively young, and further positive developments have to be expected. Some will simply aim at a continuous improvement of image quality and workflow, others will be directed at technological advances or concepts. Most important, and partly dependent on the above, are the development and improvement of applications. We here try and list some options and possibilities, again without a claim of completeness.

Developments in detector technology are likely and they bear the potential for significant improvements of FD-CT. Faster and flexible detector read-out allowing for faster scanning is a primary goal. Direct converters, alluded to earlier, would allow for higher inherent spatial resolution, since the degrading effect of light transmission will be omitted. This will also allow for higher absorber thickness and for absorber materials with higher absorption efficiency, such as mercuric iodide. Energy-selective readout and photon-counting modes are further options that will allow for dual-energy imaging and for higher dose efficiency [54, 55].

Computer-assisted interventions and operations will increase in frequency and in importance, as they provide higher precision and higher result quality. It is not only the difficult cases in interventions or operations which profit from the support by 3D image-guided planning and guidance by navigation systems [56, 57]. Robotics will play an increasing role both for imaging and for therapy. Figure 8 shows a respective scenario of an interventional suite in the future, which may appear totally fictitious but, in our opinion, is likely to appear. A large robot, either floor- or ceiling-mounted, moves the C-arm system at a speed and with mechanical precision higher than available today; fast and versatile imaging concepts are the motivation here. A second floor-mounted robot holds the patient bed and allows positioning of the patient with higher versatility, e.g. adapting table height, swivel and inclination

with higher flexibility than available at present; the respective technology is already under evaluation for high-precision radiation and particle therapy. An additional small robot mounted to the patient bed, on demand, will support the interventional radiologist and the surgeon in positioning devices or implants; the respective technology is already under evaluation in the field of computer-assisted surgery.

The introduction of dual-source systems to clinical CT in 2005 [13, 58], which provided higher X-ray power and shorter effective scan times, may also be an option for C-arm systems. Bi-plane systems are already used routinely. Set-ups where both systems follow the same trajectory are possible technically. Controlling the position of devices or instruments using triangulation principles with two simultaneously acquired projections would be one application example in 2D mode; very fast measurement to enable intra-operative perfusion measurements in 3D CT mode would be a further one. We will have to wait and monitor how FD-CT applications develop and establish themselves. The necessary technological support will become available.

Conclusions

FD-CT has gained recognition and acceptance as a dedicated application-specific CT implementation within a remarkably short time-span. Interventional and intra-operative imaging are most important at present, but quite a number of further FD-CT applications are on the horizon. In all cases, the application-related advantages outweigh the image quality-related disadvantages, which still have to be acknowledged when comparing FD-CT to clinical CT. There is good reason, though, to expect that technological advances will help to improve FD-CT significantly in the future. Detector technology will play a key role here.

FD-CT does not aim to challenge standard diagnostic CT, but will gain great importance in future radiology providing applications for planning, guiding, monitoring and assessing interventional procedures and image-guided therapy in general. Its versatility, e.g. the very efficient way of combining 2D fluoroscopic and 3D CT imaging in one unit, is a decisive advantage. And, by the way, in that sense FD-CT also constitutes a new and promising form of 2D/3D combination imaging.

Acknowledgements We would like to sincerely thank Arnd Doerfler and Marek Karolczak for a careful review of the manuscript and many helpful discussions. Figure 6a is courtesy of Reinhard Loose, Nürnberg and Fig. 6b, c courtesy of Arnd Doerfler, Dept. of Neuroradiology, University Erlangen-Nuremberg.

References

1. Fahrig R, Fox S, Lownie S, Holdsworth DW (1997) Use of a C-arm system to generate true 3-D computed rotational angiograms: Preliminary in vitro and in vivo results. AJNR Am J Neuroradiol 18(8):1507–1514
2. Grass M, Koppe E, Klotz E, Proksa R, Kuhn H, Aerts J, Op de Beek J, Kemkers R (1999) Three-dimensional reconstruction of high contrast objects using C-arm image intensifier projection data. Comput Med Imaging Graph 23:311–321
3. Fahrig R, Holdsworth DW (2000) Three-dimensional computed tomographic reconstruction using a C-arm mounted XRII: image-based correction of gantry motion nonidealities. Med Phys 27:30–38
4. Linsenmaier U, Rock C, Euler E, Wirth S, Brandl R, Kotsianos D, Mutschler M, Pfeifer KJ (2002) Three-dimensional CT with a modified C-arm image intensifier: feasibility. Radiology 224 (1):286–292
5. Jaffray DA, Siewerdsen JH (2000) Cone-beam computed tomography with a flat-panel imager: initial performance characterization. Med Phys 27 (7):1311–1323
6. Ning R, Chen B, Yu R, Conover D, Tang X, Ning Y (2000) Flat-panel detector-based cone-beam volume CT angiography imaging: system evaluation. IEEE Trans Med Imag 19 (9):949–963
7. Groh BA, Siewerdsen JH, Drake DG, Wong JW, Jaffray DA (2002) A performance comparison of flat-panel imager-based MV and kV cone-beam CT. Med Phys 29(6):967–975
8. Kalender WA (2003) The use of flat-panel detectors for CT imaging. Der Einsatz von Flachbilddetektoren für die CT-Bildgebung. Der Radiologe 43:379–387
9. Jaffray DA, Siewerdsen JH, Wong J, Martinez A (2002) Flat-panel cone-beam computed tomography for image-guided radiation therapy. Int J Radiat Oncol Biol Phys 53(5): 1337–1349
10. Siewerdsen JH, Moseley D, Burch S, Bisland S, Bogaards A, Wilson B, Jaffray DA (2005) Volume CT with a flat-panel detector on a mobile, isocentric C-arm: pre-clinical investigation in guidance of minimally invasive surgery. Med Phys 32:241–254
11. Holdsworth DW, Pollmann S, Nikolov HN, Fahrig R (2005) Correction of XRII geometric distortion using a liquid-filled grid and image subtraction. Med Phys 32:55–64
12. Fahrig R, Dixon RL, Payne T, Morin L, Ganguly A (2006) Dose and image quality for a cone-beam C-arm CT system. Med Phys 33(12):4541–4550
13. Kalender WA (2005) Computed tomography. Fundamentals, system technology, image quality, applications, 2nd (edn). Publicis, Erlangen
14. Zellerhof M, Scholz B, Rührnschopf E, Brunner T (2005) Low contrast 3D-reconstruction from C-arm data. Progress Biom. Opt Imag Proc SPIE 5745 (I):646–655

15. Saunders R Jr, Samei E, Jesneck J, Lo J (2005) Physical characterization of a prototype selenium-based full field digital mammography detector. Med Phys 32:588–599
16. Kang Y, Antonuk LE, El-Mohri Y, Hu L, Li Y, Sawant A, Su Z, Wang Y, Yamamoto J, Zhao Q (2005) Examination of PbI2 and HgI2 photonconductive materials for direct detection, active matrix, flat-panel imagers for diagnostic X-ray imaging. IEEE Trans Nuclear Science 52:38–45
17. Zentai G, Schieber M, Partain L, Pavlyuchkova R, Proano C (2005) Large area mercuric iodide and lead iodide X-ray detectors for medical and non-destructive industrial imaging. J Crystal Growth 275:e1327–e1331
18. Bloomquist A, Yaffe M, Mawdsley G, Hunter D, Beideck D (2006) Lag and ghosting in a clinical flat-panel selenium digital mammography system. Med Phys 33:2998–3005
19. Zhao W, DeCrescenzo G, Kasap S, Rowlands J (2005) Ghosting caused by bulk charge trapping in direct conversion flat-panel detectors using amorphous selenium. Med Phys 32:488–500
20. Antonuk L, Jee KW, El-Mohri Y, Maolinbay M, Nassif S, Rong X, Zhao Q, Siewerdsen JH, Street RA, Shah KS (2000) Strategies to improve the signal and noise performance of active matrix, flat-panel imagers for diagnostic x-ray applications. Med Phys 27(2):289–306
21. Siewerdsen JH, Jaffray DA (1999) Cone-beam computed tomography with a flat-panel imager: effects of image lag. Med Phys 26(12):2635–2647
22. Siewerdsen JH, Jaffray DA (1999) A ghost story: spatio-temporal response characteristics of an indirect-detection flat-panel imager. Med Phys 26:1624–1641
23. Kachelrieß M, Schaller S, Kalender WA (2000) Advanced single-slice rebinning in cone-beam spiral CT. Med Phys 27(4):754–772
24. Feldkamp LA, Davis LC, Kress JW (1984) Practical cone-beam algorithm. J Optical Society America A 1(6):612–619
25. Mori S, Endo M, Obata T, Tsunoo T, Susumu K, Tanada S (2006) Properties of the prototype 256-row (cone beam) CT scanner. Eur Radiol 16:2100–2108
26. Shope TB, Gagne RM, Johnson GC (1981) A method for describing the doses delivered by transmission x-ray computed tomography. Med Phys 8:488–495
27. Dixon RL (2003) A new look at CT dose measurement: beyond CTDI. Med Phys 30(6):1272–1280
28. Dixon RL, Munley MT, Bayram E (2005) An improved analytical model for CT dose simulation with a new look at the theory of CT dose. Med Phys 32 (12):3712–3728
29. Nakonechny KD, Fallone BG, Rathee S (2005) Novel methods of measuring single scan dose profiles and cumulative dose in CT. Med Phys 32:98–109
30. Schmidt B, Kalender WA (2002) A fast voxel-based Monte Carlo method for scanner- and patient-specific dose calculations in computed tomography. Physica Medica XVIII(2):43–53
31. Ohnesorge B, Flohr T, Schwarz K, Heiken JP, Bae KT (2000) Efficient correction for CT image artifacts caused by objects extending outside the scan field of view. Med Phys 27(1):39–46
32. Sourbelle K, Kachelriess M, Kalender WA (2005) Reconstruction from truncated projections in CT using adaptive detruncation. Eur Radiol 15(5):1008–1014
33. Endo M, Tsunoo T, Nakamori N, Yoshida K (2001) Effect of scattered radiation on image noise in cone beam CT. Med Phys 28(4):469–474
34. Siewerdsen JH, Jaffray DA (2001) Cone-beam computed tomography with a flat-panel imager: magnitude and effects of x-ray scatter. Med Phys 28 (2):220–231
35. Kyriakou Y, Riedel T, Kalender WA (2006) Combining deterministic and Monte Carlo calculations for fast estimation of scatter intensities in CT. Phys Med Biol 51:4567–4586
36. Sharpe MB, Moseley DJ, Purdie TG, Islam M, Siewerdsen JH, Jaffray DA (2006) The stability of mechanical calibration for a kV cone beam computed tomography system integrated with linear accelerator. Med Phys 33 (1):136–144
37. Rougee A, Picard C, Ponchut C, Trousset Y (1993) Geometrical calibration of X-ray imaging chains for three-dimensional reconstruction. Comput Med Imaging Graph 17 (4/5):295–300
38. Smekal von L, Kachelrieß M, Stepina E, Kalender WA (2004) Geometric misalignment and calibration in cone-beam tomography. Med Phys 31 (12):3242–3266
39. Mitschke M, Navab N (2000) Optimal configuration for dynamic calibration of projection geometry of x-ray C-arm systems. IEEE Workshop on Mathematical Methods in Biomedical Image Analysis (MMBIA)
40. Benndorf G, Strother CM, Claus B, Naeini R, Morsi H, Mawad ME (2005) Angiographic CT in cerebrovascular stenting. AJNR Am J Neuroradiol 26 (7):1813–1818
41. Doerfler A, Wanke I, Egelhof T, Dietrich U, Asgari S, Stolke D, Forsting M (2001) Aneurysmal rupture during embolization with Guglielmi Detachable Coils: causes, management, and outcome. AJNR Am J Neuroradiol 22:1825–1832
42. Heran NS, Song JK, Namba K, Smith W, Niimi Y, Berenstein A (2006) The utility of DynaCT in neuroendovascular procedures. AJNR Am J Neuroradiol 27(2):330–332
43. Lachaine M, Fourkal E, Fallone B (2001) Investigation into the physical characteristics of active matrix flat panel imagers for radiotherapy. Med Phys 28:1689–1695
44. Pang G, Rowlands J (2004) Development of high quantum efficiency, flat panel, thick detectors for megavoltage x-ray imaging: a novel direct-conversion design and its feasibility. Med Phys 31:3004–3016
45. Schulze D, Heiland H, Thurmann H, Adam G (2004) Radiation exposure during midfacial imaging using 4- and 16-slice computed tomography, cone beam computed tomography systems and conventional radiography. Dentomaxillofac Radiol 33:83–86
46. Chang C, Sibala J, Lin F, Jewell W, Templeton A (1978) Preoperative diagnosis of potentially precancerous breast lesions by computed tomography breast scanner: preliminary study. Radiology 129:209–210
47. Boone J, Kwan A, Seibert JA, Shah N, Lindfors K, Nelson T (2005) Technique factors and their relationship to radiation dose in pendant geometry breast CT. Med Phys 32:3767–3776
48. Boone J, Nelson T, Lindfors K, Seibert JA (2001) Dedicated breast CT: radiation dose and image quality evaluation. Radiology 221(3):657–667
49. Vollmar S, Kalender WA (2007) Breast CT at the same exposure level as in two-view mammography yields excellent image quality. Eur Radiol Suppl. (ECR 2007; B–397): in press
50. Gupta R, Grasruck M, Suess C, Bartling S, Schmidt B, Stierstorfer K, Popescu S, Brady S, Flohr T (2006) Ultra-high resolution flat-panel volume CT: fundamental principles, design architecture, and system characterization. Eur Radiol 33:1612–1622
51. Mahnken A, Seyfarth T, Flohr T, Herzog C, Stahl J, Stanzel S, Kuettner A, Wildberger J, Guenther R (2005) Flat-panel detector computed tomography for the assessment of coronary artery stents: phantom study in comparison with 16-slice spiral computed tomography. Invest Radiol 40:8–13

52. Kiessling F, Greschuss S, Lichy MP, Bock M, Fink C, Vosseler S, Moll J, Mueller MM, Fusening NE, Traupe H, Semmler W (2004) Volumetric computed tomography (VCT): a new technology for non-invasive, high-resolution monitoring of tumor angiogenesis. Nat Med 10(10):1133–1138
53. Ross W, Cody Dd, Hazle JD (2006) Design and performance characteristics of a digital flat-panel computed tomography system. Med Phys 33:1888–1901
54. Richard S, Siewerdsen JH, Jaffray DA, Moseley D, Bakhtiar B (2005) Generalized DQE analysis of radiographic and dual-energy imaging using flat-panel detectors. Med Phys 32:1397–1413
55. Xu T, Ducote J, Wong J, Molloi S (2006) Feasibility of real time dual-energy imaging based on a flat panel detector for coronary artery calcium quantification. Med Phys 33:1612–1622
56. Daly MJ, Siewerdsen JH, Moseley D, Jaffray DA, Irish JC (2006) Intraoperative cone-beam CT for guidance of head and neck surgery: assessment of dose and image quality using a C-arm prototype. Med Phys 33:3767–3780
57. Nagel M (2006) Bildbasierte, computerunterstützte Navigation für die interventionelle Radiologie. Thesis at the Institute of Medical Physics, Friedrich-Alexander-University Erlangen-Nürnberg
58. Flohr T, McCollough CH, Bruder H, Petersilka M, Gruber K, Süß C, Grasruck M, Stierstorfer K, Krauss B, Raupach R, Primak N, Küttner A, Achenbach S, Becker C, Kopp A, Ohnesorge B (2006) First performance of a dual-source CT (DSCT) system. Eur Radiol 16:256–268